

Synthesis, Characterization, Luminescence, and Non-linear Optical Properties of Oxadiazole- and Truxene-Containing Platinum(II) Alkynyl Complexes with Donor–Acceptor Functionalities

Carmen Ka Man Chan,[†] Chi-Hang Tao,[†] Hoi-Lam Tam,[‡] Nianyong Zhu,[†] Vivian Wing-Wah Yam,^{*†} and Kok-Wai Cheah^{*‡}

Centre for Carbon-Rich Molecular and Nano-Scale Metal-Based Materials Research and Department of Chemistry, The University of Hong Kong, Pokfulam Road, Hong Kong, P.R. China, and Centre for Advanced Luminescence Materials, Hong Kong Baptist University and Department of Physics, Hong Kong Baptist University, Hong Kong, P.R. China

Received September 19, 2008

A series of luminescent platinum(II) alkynyl complexes containing 2,5-diphenyl-1,3,4-oxadiazole (oxa-2,5) and 10,15-dihydro-5H-diindeno[1,2-a;1',2'-c]fluorene (truxene) as the cores and different electron donors at the periphery has been synthesized and characterized. These complexes showed long-lived emissions in both solution and in the solid state at room temperature and have been found to exhibit two-photon absorption (2PA) and two-photon induced luminescence. Their 2PA cross-sections (σ_2) have also been determined.

Introduction

There has been a growing interest in the development of two-photon absorbing materials because of their various applications, such as in optical data storage,^{1–3} frequency upconverted lasing,^{4–7} three-dimensional microfabrication,^{8,9} fluorescence imaging,^{10–12} non-linear photonics,¹³ and pho-

todynamic therapy.^{14,15} To obtain materials with large two-photon absorption (2PA) cross-sections, the design and synthesis of chromophores or dendrimers with large differences in polarization upon excitation and extended π -conjugation within the molecule have received much attention.¹⁶ Large changes in polarization can be achieved through various structural motifs, such as donor– π –acceptor, donor– π –donor, acceptor– π –acceptor, donor–acceptor–donor or acceptor–donor–acceptor, which have been found to display remarkable improvements in 2PA capabilities.

Extended π -conjugated and star-shaped molecules have shown interesting properties, such as conducting, optical, non-linear optical and electroluminescent properties.^{17–23} In particular, 2,5-diphenyl-1,3,4-oxadiazole (oxa-2,5) and 10,15-

* To whom correspondence should be addressed. E-mail: wwyam@hku.hk (V.W.-W.Y.), kwcheah@hkbu.edu.hk (K.-W.C.). Fax: 852 2857 1586 (V.W.-W.Y.). Phone: 852 2859 2153 (V.W.-W.Y.), 852 3411 7033 (K.-W.C.).

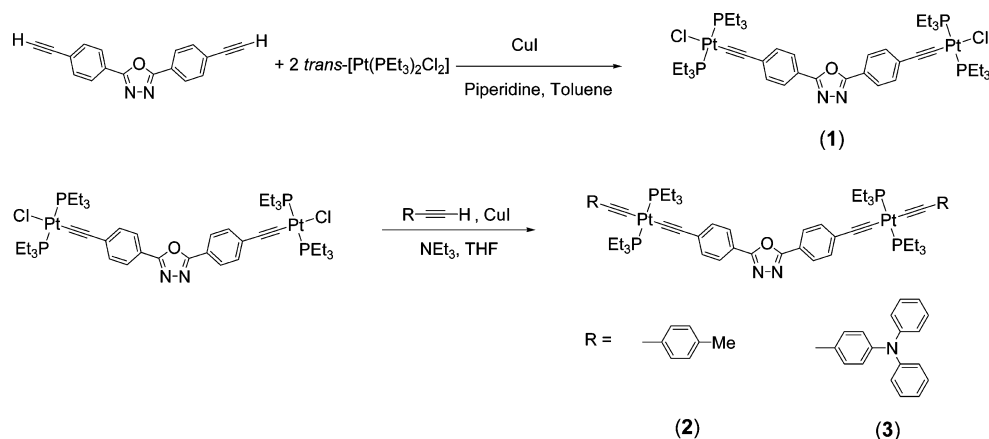
[†] The University of Hong Kong.

[‡] Hong Kong Baptist University.

- (1) Parthenopoulos, D. A.; Rentzepis, P. M. *Science* **1989**, *249*, 843.
- (2) Strickler, J. H.; Webb, W. W. *Adv. Mater.* **1993**, *5*, 479.
- (3) He, G. S.; Gvishi, R.; Prasad, P. N.; Reinhardt, B. A. *Opt. Commun.* **1995**, *117*, 133.
- (4) Mukherjee, A. *Appl. Phys. Lett.* **1993**, *62*, 3423.
- (5) Zheng, Q.; He, G. S.; Lin, T.-C.; Prasad, P. N. *J. Mater. Chem.* **2003**, *13*, 2499.
- (6) He, G. S.; Zhao, C. F.; Bhawalkar, J. D. *Appl. Phys. Lett.* **1995**, *78*, 3703.
- (7) Zhao, C. F.; He, G. S.; Bhawalkar, J. D.; Park, C. K.; Prasad, P. N. *Chem. Mater.* **1995**, *7*, 1979.
- (8) Kawata, S.; Sun, H. B.; Tanaka, T.; Takada, K. *Nature* **2001**, *412*, 697.
- (9) Cumpston, B. H.; Ananthavel, S. P.; Barlow, S.; Dyer, D. L.; Ehrlich, J. E.; Erskine, L. L.; Heikal, A. A.; Kuebler, S. M.; Lee, S. I.-Y.; McCord-Maughon, D.; Qin, J.; Rockel, H.; Rumi, M.; Wu, X.-L.; Marder, S. R.; Perry, J. W. *Nature* **1999**, *398*, 51.
- (10) Denk, W.; Strickler, J. H.; Webb, W. W. *Science* **1990**, *248*, 73.
- (11) Belfield, K. D.; Schafer, K. J.; Liu, Y.; Liu, J.; Ren, X.; Van Stryland, E. W. *J. Phys. Org. Chem.* **2000**, *13*, 837.
- (12) Gu, M.; Tannous, T.; Sheppard, C. J. R. *Opt. Commun.* **1995**, *117*, 406.

- (13) He, G. S.; Bhawalkar, J. D.; Zhao, C. F.; Prasad, P. N. *Appl. Phys. Lett.* **1995**, *67*, 2433.
- (14) Bhawalkar, J. D.; Kumar, N. D.; Zhao, C. F.; Prasad, P. N. *J. Clin. Laser Med. Surg.* **1997**, *15*, 201.
- (15) Frederiksen, P. K.; Jørgensen, M.; Ogilby, P. R. *J. Am. Chem. Soc.* **2001**, *123*, 1215.
- (16) Albota, M.; Beljonne, D.; Brédas, J.-L.; Ehrlich, J. E.; Fu, J.-Y.; Heikal, A. A.; Hess, S. E.; Kogej, T.; Levin, M. D.; Marder, S. R.; McCord-Maughon, D.; Perry, J. W.; Rockel, H.; Rumi, M.; Subramaniam, G.; Webb, W. W.; Wu, X.-L.; Xu, C. *Science* **1998**, *281*, 1653.
- (17) Huang, P.-H.; Shen, J.-Y.; Pu, S.-C.; Wen, Y.-S.; Lin, J. T.; Chou, P.-T.; Yeh, M.-C. P. *J. Mater. Chem.* **2006**, *16*, 850.
- (18) Shao, P.; Huang, B.; Chen, L.; Liu, Z.; Qin, J.; Gong, H.; Ding, S.; Wang, Q. *J. Mater. Chem.* **2005**, *15*, 4502.
- (19) Shao, P.; Li, Z.; Qin, J.; Gong, H.; Ding, S.; Wang, Q. *Aust. J. Chem.* **2006**, *59*, 49.
- (20) Zheng, Q.; He, G. S.; Prasad, P. N. *Chem. Mater.* **2005**, *17*, 6004.

Scheme 1. Synthesis of Oxadiazole-Containing Dinuclear Platinum(II) Complexes



dihydro-5*H*-diindeno[1,2-*a*;1',2'-*c*]fluorene (truxene) appear to be promising building blocks for the construction of functional materials because of their rigid structures, good thermal and chemical stabilities, and relatively high luminescence quantum yields.^{17–25} In addition, the electron-deficient nature of 2,5-diphenyl-1,3,4-oxadiazole (oxa-2,5) has fostered its applications as electron-acceptors in the development of 2PA chromophores.

Besides, symmetrical D- π -A- π -D or A- π -D- π -A molecules have been shown to exhibit relatively large 2PA cross-sections. Works by various research groups have reported that dendritic or branched molecules showed enhanced 2PA because of an extended π -conjugation and an increased intramolecular charge redistribution compared to singly branched dipolar chromophores.^{18–20}

Apart from the studies of organic compounds for 2PA, there has been a growing interest in the study of metal complexes for non-linear optical applications in recent years.^{26–34} Some organotransition metal complexes, such as ferrocenyl, nickel(II), ruthenium(II), manganese(I), and gold(I), have been reported by various research groups to show interesting non-linear optical properties.^{26–34} Recent

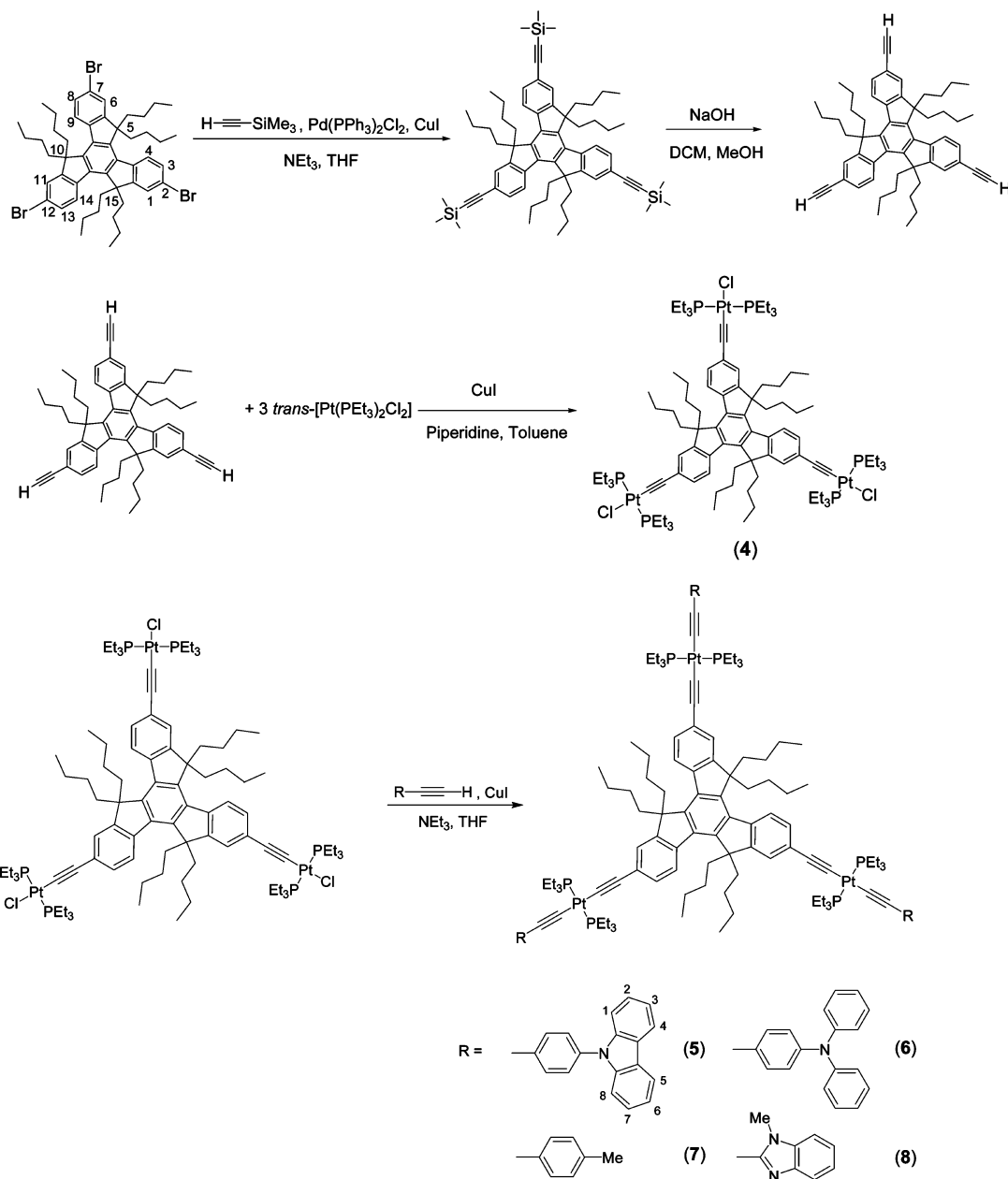
works have shown that metal alkynyls, through the stability of the metal-carbon bond and the $d\pi$ - $p\pi$ overlap, might serve as promising structural motifs for the construction of optical limiting, second harmonic generating, two-photon absorbing, and two-photon induced luminescence materials.^{35–38} In particular, a series of thienylalkynyl complexes of platinum(II) with dendronized end-groups has been found to exhibit σ_2 in the range of 5–10 GM and was also found to show optical limiting properties.^{39,40}

Although organic chromophores with oxa-2,5^{17–19} and truxene^{20–25} have been synthesized, the construction of carbon-rich metal-containing complexes containing these core ligands has been much less explored.^{41–43} With our recent interests and efforts in the design and synthesis of linear and branched luminescent metal alkynyl complexes,^{44–50} a program was launched to explore the employment of the truxene and oxadiazole functionalities in the construction of metal alkynyl complexes. The photophysical and the 2PA properties have also been studied. Herein are described the design, synthesis, characterization, and luminescence behavior of a series of branched platinum(II) alkynyl complexes containing oxa-2,5 and truxene as the core and various electron-donating groups, such as triphenylamine and carbazole, as the peripheral units. The structure of triethynylhexabutyltruxene has also been determined.

- (21) Pei, J.; Wang, J.-L.; Cao, X.-Y.; Zhou, X.-H.; Zhang, W.-B. *J. Am. Chem. Soc.* **2003**, *125*, 9544.
- (22) Kanibolotsky, A. L.; Berrifge, R.; Skabara, P. J.; Perepichka, I. F.; Bradley, D. D. C.; Koeberg, M. J. *Am. Chem. Soc.* **2004**, *126*, 13695.
- (23) Cao, X.-Y.; Liu, X.-H.; Zhou, X.-H.; Zhang, Y.; Jiang, Y.; Cao, Y.; Cui, Y.-X.; Pei, J. *J. Org. Chem.* **2004**, *69*, 6050.
- (24) Zhang, W.-B.; Jin, W.-H.; Zhou, X.-H.; Pei, J. *Tetrahedron* **2007**, *63*, 2907.
- (25) Yuan, M.-S.; Liu, Z.-Q.; Fang, Q. *J. Org. Chem.* **2007**, *72*, 7915.
- (26) Green, M. L. H.; Marder, S. R.; Thompson, M. E.; Bandy, J. A.; Bloor, D.; Kolinsky, P. V.; Jones, R. J. *Nature* **1987**, *330*, 360.
- (27) Green, M. L. H.; Qin, J.; O'Hare, D.; Bunting, H. E.; Thompson, M. E.; Marder, S. R.; Chatakonda, K. *Pure Appl. Chem.* **1989**, *61*, 817.
- (28) Bandy, J. A.; Bunting, H. E.; Garcia, M. H.; Green, M. L. H.; Marder, S. R.; Thompson, M. E.; Bloor, D.; Kolinsky, P. V.; Jones, R. J.; Perry, J. W. *Polyhedron* **1992**, *11*, 1429.
- (29) Bunting, H. E.; Green, M. L. H.; Marder, S. R.; Thompson, M. E.; Bloor, D.; Kolinsky, P. V.; Jones, R. J. *Polyhedron* **1992**, *11*, 1489.
- (30) Barlow, S.; Marder, S. R. *Chem. Commun.* **2000**, 1555.
- (31) Davies, S. J.; Johnson, B. F. G.; Lewis, J.; Muhammad, S. J. *Organomet. Chem.* **1991**, *401*, C43.
- (32) Colbert, M. C. B.; Edwards, A. J.; Lewis, J.; Long, N. J.; Page, N. A.; Parker, D. G.; Raithby, P. R. *J. Chem. Soc., Dalton Trans.* **1994**, *17*, 2589.
- (33) McDonagh, A. M.; Humphrey, M. G.; Samoc, M.; Luther-Davies, B. *Organometallics* **1999**, *18*, 5195.
- (34) Powell, C. E.; Humphrey, M. G. *Coord. Chem. Rev.* **2004**, *248*, 725.

- (35) McKay, T. J.; Staromlynska, J.; Wilson, P. *J. Appl. Phys.* **1999**, *85*, 1337.
- (36) Rogers, J. E.; Slagle, J. E.; Krein, D. M.; Burke, A. R.; Hall, B. C.; Fratini, A.; McLean, D. G.; Fleitz, P. A.; Cooper, T. M.; Drobizhev, M.; Makarov, N. S.; Rebane, A.; Kim, K.-Y.; Farley, R.; Schanze, K. S. *Inorg. Chem.* **2007**, *46*, 6483.
- (37) Jiang, F.-L.; Wong, W.-K.; Zhu, X.-J.; Zhou, G.-J.; Wong, W.-Y.; Wu, P.-L.; Tam, H.-L.; Cheah, K.-W.; Ye, C.; Liu, Y. *Eur. J. Inorg. Chem.* **2007**, 3365.
- (38) Tao, C.-H.; Yang, H.; Zhu, N.; Yam, V. W.-W.; Xu, S.-J. *Organometallics* **2008**, *27*, 5453.
- (39) Glimsdal, E.; Carlsson, M.; Eliasson, B.; Minaev, B.; Lindgren, M. J. *Phys. Chem. A* **2007**, *111*, 244.
- (40) Westlund, R.; Glimsdal, E.; Lindgren, M.; Vestberg, R.; Hawker, C.; Lopez, C.; Malmström, E. *J. Mater. Chem.* **2008**, *18*, 166.
- (41) He, Z.; Wong, W.-Y.; Yu, X.; Kwok, H.-S.; Lin, Z. *Inorg. Chem.* **2006**, *45*, 10922.
- (42) Lu, W.; Law, Y.-C.; Han, J.; Chui, S. S.-Y.; Ma, D.-L.; Zhu, N.; Che, C.-M. *Chem. Asian J.* **2008**, *3*, 59.
- (43) Tisch, T. L.; Lynch, T. J.; Dominguez, R. *J. Organomet. Chem.* **1989**, *377*, 265.

Scheme 2. Synthesis of Truxene-Containing Trinuclear Platinum(II) Complexes



Results and Discussion

Synthesis and Characterization. The targeted branched dinuclear and trinuclear platinum(II) complexes were synthesized according to Scheme 1 and Scheme 2, respectively. Chloroplatinum(II) complexes **1** and **4** were obtained by modification of the preparation of the related trinuclear platinum(II) complexes which were reported

previously by our group.^{45,49} These complexes were prepared in refluxing toluene and piperidine in the presence of a catalytic amount of CuI and an excess of $\text{trans-[Pt(PEt}_3)_2\text{Cl}_2]$ to minimize the formation of undesirable oligomeric materials. The branched platinum(II) bis-alkynyl complexes **2**, **3**, **5–8** were synthesized using a copper(I)-catalyzed dehydrohalogenation approach with the corresponding multinuclear complex precursors **1** and **4**. Complexes **2**, **3**, **5–8** were obtained in reasonable yields with different alkynyl ligands, which demonstrated that precursor complexes **1** and **4** are versatile starting materials for the syntheses of luminescent branched carbon-rich metal-containing materials.

(44) Yam, V. W.-W.; Zhang, L.; Tao, C.-H.; Wong, K. M.-C.; Cheung, K.-K. *J. Chem. Soc., Dalton Trans.* **2001**, 1111.

(45) Yam, V. W.-W.; Tao, C.-H.; Zhang, L.; Wong, K. M.-C.; Cheung, K.-K. *Organometallics* **2001**, *20*, 453.

(46) Yam, V. W.-W.; Wong, K. M.-C.; Chong, S. H.-F.; Lau, V. C.-Y.; Lam, S. C.-F.; Zhang, L.; Cheung, K.-K. *J. Organomet. Chem.* **2003**, *670*, 205.

(47) Tao, C.-H.; Wong, K. M.-C.; Zhu, N.; Yam, V. W.-W. *New J. Chem.* **2003**, *27*, 150.

(48) Chong, S. H.-F.; Lam, S. C.-F.; Yam, V. W.-W.; Zhu, N.; Cheung, K.-K. *Organometallics* **2004**, *23*, 4924.

(49) Tao, C.-H.; Zhu, N.; Yam, V. W.-W. *Chem.—Eur. J.* **2005**, *11*, 1647; *Chem.—Eur. J.* **2008**, *14*, 1377.

(50) Lam, S. C.-F.; Yam, V. W.-W.; Wong, K. M.-C.; Cheng, E. C.-C.; Zhu, N. *Organometallics* **2005**, *24*, 4298.

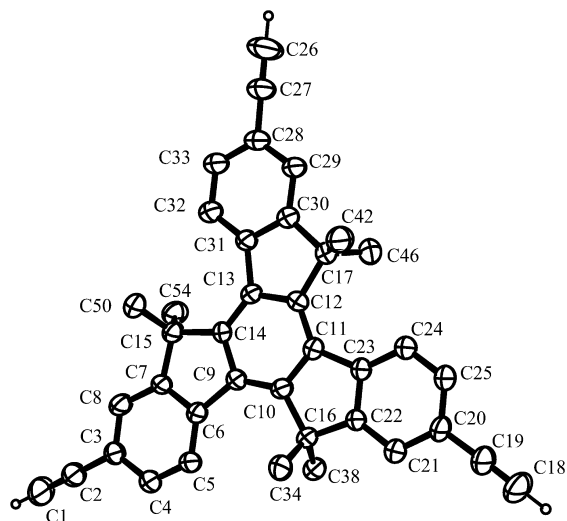


Figure 1. Perspective view of triethynylhexabutyltruxene with atomic numbering scheme. Only the *ipso*-carbons of the butyl chains were shown. Hydrogen atoms (except the acetylenic hydrogens) have been omitted for clarity. Thermal ellipsoids were shown at the 30% probability level.

Table 1. Selected Bond Lengths [Å] and Bond Angles [deg] for Triethynylhexabutyltruxene with Estimated Standard Deviations in Parentheses

Selected Bond Lengths [Å]			
C(1)–C(2)	1.179(5)	C(18)–C(19)	1.174(5)
C(26)–C(27)	1.147(5)		
Selected Bond Angles [deg]			
C(1)–C(2)–C(3)	178.2(7)	C(18)–C(19)–C(20)	178.5(6)
C(26)–C(27)–C(28)	176.4(6)	C(50)–C(15)–C(54)	111.5(3)
C(42)–C(17)–C(46)	113.0(4)	C(34)–C(16)–C(38)	111.3(3)

All the complexes have been characterized by IR, positive FAB-MS, ^1H and $^{31}\text{P}\{^1\text{H}\}$ NMR spectroscopy and gave satisfactory elemental analyses. The ^{31}P NMR spectra of complexes **1**–**8** all showed a singlet signal, which is indicative of the highly symmetrical structure of the molecules, in the range of δ 14.8–15.1 ppm for the precursor chloro complexes **1** and **4** and δ 11.0–11.7 ppm for the other alkynyl complexes. Platinum satellites with $J_{\text{Pt-P}} \sim 2300$ Hz were observed in all the branched complexes which are characteristic of a *trans*-P–Pt–P configuration.⁵¹

Crystal Structure Determination. Figure 1 shows the perspective drawing of triethynylhexabutyltruxene, and the selected bond lengths and angles are given in Table 1. Only the *ipso* carbons on the butyl chains are shown in the figure. The C≡C bond lengths of the three peripheral alkynes lie in the range of 1.147–1.179 Å. The bond angles about the sp hybridized carbons are close to the ideal value of 180°. As shown in Figure 1, the truxene backbone is nearly coplanar with six butyl chains lying out of the aromatic plane which is expected for the sp³ hybridized carbons C15, C16, and C17. As a result of the presence of these butyl chains protruding from the planes of the truxene backbone, π stacking does not exist, and the six butyl chains also served to enhance the solubility of the molecule.

Electronic Absorption and Emission. The electronic absorption spectra of these dinuclear and trinuclear platinum-

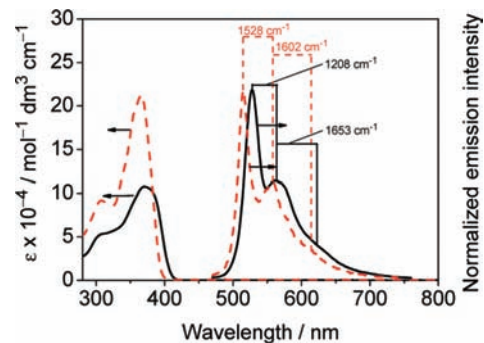


Figure 2. Electronic absorption (left) and normalized emission spectra (right) of complexes **3** (solid black line) and **6** (red dashed line) in benzene at room temperature.

Table 2. Electronic Absorption and Photophysical Data for Complexes **1**–**8**

complex	λ_{abs} [nm] (ϵ [dm ³ mol ⁻¹ cm ⁻¹]) ^a	medium (T [K])	λ_{em} [nm] (τ_0 [μs])	Φ_{lum}^d
1	362 (65790)	C ₆ H ₆ (298)	^c	^e
		solid (298)	^c	
		solid (77)	527 (170)	
2	370 (106100)	glass (77) ^b	518 (380)	0.17
		C ₆ H ₆ (298)	528 (80)	
		solid (298)	532 (4.6)	
3	308 sh (53250), 370 (107990)	solid (77)	533 (80)	0.20
		glass (77) ^b	520 (420)	
		C ₆ H ₆ (298)	528 (32)	
4	316 (55100), 352 (148700)	solid (298)	529 (6.0)	0.10
		solid (77)	528 (280)	
		glass (77) ^b	520 (320)	
5	354 (197200), 362 sh (183800)	C ₆ H ₆ (298)	528 (280)	0.13
		solid (77)	522 (110)	
		glass (77) ^b	509 (700)	
6	306 (91700), 366 (212900)	C ₆ H ₆ (298)	515 (45)	0.10
		solid (298)	519 (6.0)	
		solid (77)	522 (52)	
7	354 (178300), 364 (171800)	glass (77) ^b	508 (550)	0.08
		C ₆ H ₆ (298)	515 (22)	
		solid (298)	522 (4.8)	
8	352 (261100), 362 (251200)	solid (77)	521 (120)	0.08
		glass (77) ^b	510 (700)	
		C ₆ H ₆ (298)	514 (56)	
		solid (298)	518 (5.5)	
		solid (77)	519 (75)	
		glass (77) ^b	508 (730)	

^a Measured in C₆H₆ at 298 K. ^b Measured in EtOH–MeOH (4:1, v/v) glass. ^c Non-emissive. ^d The luminescence quantum yield, measured at room temperature using quinine sulfate in 1.0 N H₂SO₄ as the reference (excitation wavelength = 365 nm, $\Phi_{\text{lum}} = 0.55$). ^e Not determined.

m(II) complexes showed intense absorption bands at about 352–370 nm with extinction coefficients of the order of 10⁴–10⁵ dm³ mol⁻¹ cm⁻¹ (Figure 2). The photophysical data of complexes **1**–**8** are summarized in Table 2. With reference to previous spectroscopic studies on *trans*-[Pt(PEt₃)₂-(C≡CR)₂]₂,^{52–56} in which the absorption bands at about 300–360 nm were assigned as metal-to-alkynyl metal-to-ligand charge transfer (MLCT) transitions, the low-energy transitions in these branched complexes may also involve a metal-to-alkynyl MLCT character. In view of the rich vibronic structures and the very large extinction coefficients observed for the chloroplatinum(II) precursors **1** and **4** that are comparable to the corresponding oxadiazole and truxene

(51) Sebal, A.; Stader, C.; Wrackmeyer, B.; Bensch, W. *J. Organomet. Chem.* **1986**, *311*, 233.

alkynyl ligands, a substantial mixing of an intraligand [$\pi \rightarrow \pi^*(\text{C}\equiv\text{C})_2\text{-oxa-2,5}$ or $(\text{C}\equiv\text{C})_3\text{-truxene}$] character of the central alkynyl core unit is likely. In addition, the electronic absorption spectra of these complexes in acetone and benzene are nearly identical. These absorption bands were found to be relatively insensitive toward the polarity of the solvent, which is in accordance with the largely intraligand $\pi \rightarrow \pi^*$ character of these transitions. Therefore, the low-energy absorptions in these branched complexes are described as an admixture of IL [$\pi \rightarrow \pi^*(\text{C}\equiv\text{C})_2\text{-oxa-2,5}$ or $(\text{C}\equiv\text{C})_3\text{-truxene}$] and MLCT [$d\pi(\text{Pt}) \rightarrow \pi^*(\text{C}\equiv\text{C})_2\text{-oxa-2,5}$ or $(\text{C}\equiv\text{C})_3\text{-truxene}$] transitions with predominantly IL character. For the dinuclear complexes **2**, **3** and the trinuclear complexes **5–8**, additional absorptions due to the IL ($\pi \rightarrow \pi^*$) transitions of the peripheral alkynyl ligands may also occur at similar energies as related systems have been reported to display absorption bands in similar regions.^{52–56} However, in view of the relatively insensitive nature of the absorption energies of the dinuclear complexes **2**, **3** and trinuclear complexes **5–8** to the nature of the peripheral aryl-alkynyl ligands, the low-energy absorptions in these branched complexes are dominated by IL [$\pi \rightarrow \pi^*(\text{C}\equiv\text{C})_2\text{-oxa-2,5}$ or $(\text{C}\equiv\text{C})_3\text{-truxene}$] transitions, with mixing of MLCT [$d\pi(\text{Pt}) \rightarrow \pi^*(\text{C}\equiv\text{C})_2\text{-oxa-2,5}$ or $(\text{C}\equiv\text{C})_3\text{-truxene}$ or $\text{C}\equiv\text{CR}$] and IL [$\pi \rightarrow \pi^*(\text{C}\equiv\text{CR})$] character.

Upon excitation at $\lambda \geq 365$ nm, the branched complexes **2**, **3**, **5–8** display luminescence in deaerated benzene solutions at room temperature (Figure 2) while all the complexes exhibit luminescence at 77 K. All complexes show large Stokes shift and lifetimes in the microsecond range, which are indicative of their triplet parentage. In contrast to the non-emissive behavior of precursor complexes **1** and **4** at room temperature, the bis-alkynyl complexes **2**, **3**, **5–8** show intense yellowish green vibronically structured emission bands at room temperature, with emission maxima at about 514–520 nm that are at nearly identical wavelengths with similar vibronic structures as the emission bands of their corresponding chloroplatinum(II) precursors **1** and **4** observed at 77 K. This finding is supportive of a triplet ^3IL [$\pi \rightarrow \pi^*(\text{C}\equiv\text{C})_2\text{-oxa-2,5}$ or $(\text{C}\equiv\text{C})_3\text{-truxene}$] emission derived mainly from the central core ligands. Emissions from the ^3IL states of the peripheral alkynyl ligands were not observed since they were higher-lying in energy, indicative of a facile energy transfer process. The energy absorbed by the peripheral ligands would be transferred to the central oxadiazole or truxene emitting core through directional energy transfer. Similar findings have also been observed in other related branched platinum(II) alkynyl complexes.^{45,49} The emission spectra of complexes **2** and **3** in 77 K glass show rich vibronic structures with vibrational progressional spacings

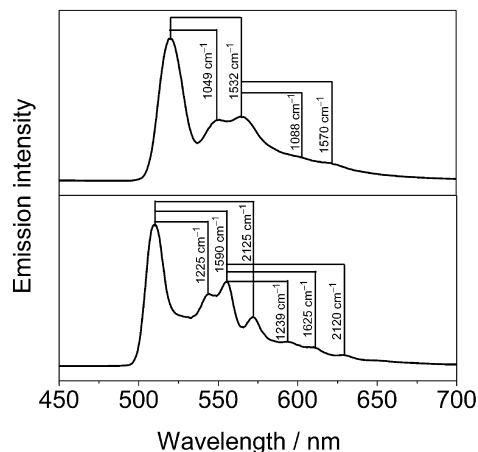


Figure 3. Emission spectra of **2** (top) and **7** (bottom) in ethanol-methanol (4:1, v/v) glass at 77 K. Excitation wavelength at 370 nm.

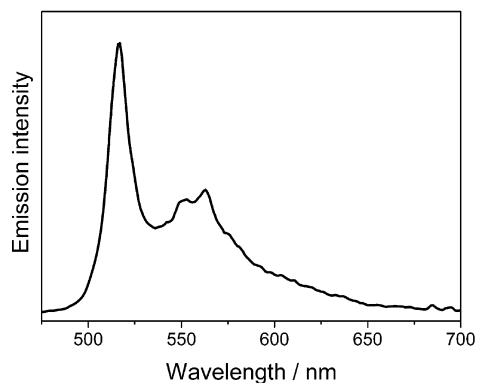


Figure 4. Two-photon induced luminescence spectrum of complex **6** in benzene at room temperature upon excitation with a mode-locked femtosecond Ti:Sapphire laser at 720 nm.

Table 3. Non-Linear Photophysical Data for Complexes **2**, **3**, **5–8**

complex	$\lambda_{\text{em}}^a/\text{nm}$ at $\lambda_{\text{ex}} = 720$ nm	σ_2/GM	power dependence
2	530	17	2.18
3	530	41	2.07
5	518	21	2.52
6	518	32	2.11
7	517	27	2.11
8	514	11	2.15

^a Measured in C_6H_6 at 298 K.

of about 1060 and 1520 cm^{-1} (Figure 3), with the former corresponding to the $\nu(\text{C}-\text{O})$ stretch and the latter to the $\nu(\text{C}=\text{C})$ and $\nu(\text{C}=\text{N})$ vibrational modes. Additional vibronic structures with progressional spacings of about 1220 and 2140 cm^{-1} from the highest energy emission band are observed for complexes **5–8** at low temperature (Figure 3), which are ascribed to the aromatic ring deformation and $\nu(\text{C}\equiv\text{C})$ vibrational modes, respectively. The emission lifetimes in solid state at room temperature are considerably shorter than that observed in dilute solutions, which may be ascribed to originate from triplet-triplet annihilation or self-quenching in the solid state.

Two-Photon Induced Luminescence (TPIL). Complexes **2**, **3**, **5–8** are found to emit in the yellowish-green region in benzene solutions upon excitation with a mode-locked femtosecond Ti:Sapphire laser at 720 nm. The TPIL spectrum of complex **6** in benzene at room temperature is shown in Figure 4. Table 3 shows the emission maxima and σ_2 at 720

- (52) Masai, H.; Sonogashira, K.; Hagihara, N. *Bull. Chem. Soc. Jpn.* **1971**, *44*, 2226.
 (53) Saksteder, L.; Baralt, E.; DeGraff, B. A.; Lukehart, C. M.; Demas, J. N. *Inorg. Chem.* **1991**, *30*, 2468.
 (54) Choi, C. L.; Cheng, Y. F.; Yip, C.; Philips, D. L.; Yam, V. W.-W. *Organometallics* **2000**, *19*, 3192.
 (55) Kwok, W. M.; Philips, D. L.; Yeung, P. K. Y.; Yam, V. W.-W. *Chem. Phys. Lett.* **1996**, *262*, 699.
 (56) Kwok, W. M.; Philips, D. L.; Yeung, P. K. Y.; Yam, V. W.-W. *J. Phys. Chem. A* **1997**, *101*, 9286.

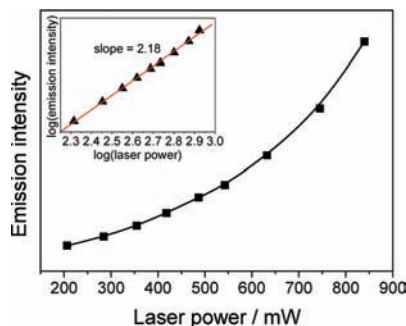


Figure 5. Power dependence of the up-converted luminescence intensity (■) of complex **2** in benzene at room temperature. The black line shows the theoretical curve for the quadratic function. The inset shows the log(emission intensity) (▲) vs log(laser power) and its linear regression (red solid line).

nm determined using TPIL. No linear absorption in the wavelength range of 500–820 nm was observed for these platinum(II) complexes, indicating that the emission induced by 720 nm excitation could not be attributed to a linear process but rather to a non-linear process. The upconverted emissions of these complexes are nearly identical to that observed in their corresponding single-photon excited emission.

The dependence of the upconverted luminescence intensities on the incident laser power was measured and the power dependence curve for complex **2** is shown in Figure 5. The inset shows the plot of log(emission intensity) versus log(laser power). A straight line plot with slope of about 2 was obtained. Since the 2PA has a quadratic dependence on intensity, the TPIL is expected to show intensity dependence on excitation. Theoretically, the log(fluorescence emission) versus log(peak laser intensity) should give a straight line with a gradient of 2.⁴⁰ Therefore, the observed quadratic dependence of the emission intensity on the incident laser power further confirms the two-photon nature of the process. The σ_2 values of these branched complexes with excitation wavelength at 720 nm have been determined using the TPIL method and are found to be in the range of 11–40 GM, which are comparable to the 5–10 GM observed in other platinum(II) alkynyl complexes of bis((4-(phenylethynyl)phenylethynyl)bis(tributylphosphine)),^{35,39,40} but smaller than that recently reported by Schanze and co-workers on some linear platinum alkynyl complexes,³⁶ which show a more extended π -conjugation in their donor- π or acceptor- π structural motifs within the alkynyl ligands.³⁶

The present study investigates the effects of the platinum(II) alkynyl π -moiety as linker on TPA in a series of platinum(II) complexes with electron-donating and electron-accepting functionalities. Through a systematic comparison study of these complexes, the σ_2 values are found to be slightly dependent on the electron-richness of the peripheral substituents while the central oxadiazole or truxene moieties have relatively small effects on the σ_2 values. In general, higher σ_2 values could be observed for complexes with relatively more electron-rich peripheral substituents. For instance, the σ_2 values of triphenylamine-containing complexes **3** and **6** are relatively higher than that of the corresponding tolyl analogues. This observation is in line with

Table 4. Electrochemical Data for Triethynylhexabutyltruxene and Complexes **1–8**^a

compound	oxidation $E_{1/2}^{b,c}$ [V versus SCE]
triethynylhexabutyltruxene	(+1.59)
1	(+1.40)
2	(+1.18)
3	+0.65, (+1.28)
4	(+1.06), (+1.28)
5	(+1.07), (+1.34), (+1.57), (+2.11)
6	+0.65, (+1.22), (+1.95)
7	(+1.15), (+1.45), (+1.81)
8	(+1.03), (+1.39), (+1.82)

^a In dichloromethane (0.1 M ⁿBu₄NPF₆); working electrode, glassy carbon; scan rate = 100 mV s⁻¹. ^b Values in parentheses refer to the anodic peak potential (E_{pa}) for the irreversible oxidation waves. ^c $E_{1/2} = (E_{pa} + E_{pc})/2$; E_{pa} and E_{pc} are the peak anodic and peak cathodic potentials, respectively.

that observed in organic 2PA chromophores.⁵⁷ The incorporation of aromatic heterocycles into the truxene system in complexes **5** and **8** did not give rise to higher σ_2 values as compared to complex **6** since the heterocycles are less electron-rich than triphenylamine, as reflected by their more positive oxidation potentials than that of triphenylamine in the cyclic voltammetric study. These findings have demonstrated that oxadiazole and truxene moieties could be building blocks for the construction of two-photon induced luminescent materials in addition to the commonly employed 1,4-diethynylbenzene. More importantly, the peripheral chloro ligands in complexes **1** and **4** would provide versatile handles for the tuning of the σ_2 values and the emission energies of these classes of complexes by the incorporation of alkynyl ligands with different electronic properties.

Electrochemical Properties. The electrochemical behavior of the complexes has been studied in dichloromethane (0.1 M ⁿBu₄NPF₆). Table 4 summarizes the electrochemical data. There is no observable reductive wave for all the complexes upon scanning up to -2.0 V, which is similar to that found in other structurally related platinum(II) alkynyl complexes.^{48,58,59} The oxidative scans of complexes **1–3** show one to two redox waves at +0.65 to +1.40 V versus saturated calomel electrode (SCE). Since there is no oxidative wave observed for 2,5-bis-(4-ethynyl)phenyl-1,3,4-oxadiazole and given the lack of peripheral alkynyl moieties in complex **1**, the irreversible waves at +1.18 to +1.40 V for complexes **1–3** are ascribed to oxidation processes that involve substantial metal-centered character. The less positive potentials for complexes **2** and **3** than their chloro precursor complex **1** are also in line with such an assignment.

Two to four irreversible waves at +1.06 to +1.22, +1.28 to +1.45, +1.57 to +1.95 and +2.11 V versus SCE were observed for complexes **4–8**. It is found that the first oxidation wave of triethynylhexabutyltruxene appears at +1.59 V, which is more positive than the first oxidation wave of complexes **4–8**, and thus an assignment of a truxene

(57) Seo, J.-W.; Jang, S. Y.; Kim, D.; Kim, H.-J. *Tetrahedron* **2008**, *64*, 2733.

(58) Younus, M.; Köhler, A.; Cron, S.; Chawdhury, N.; Al-Mandhary, M. R. A.; Khan, M. S.; Lewis, J.; Long, N. J.; Friend, R. H.; Raithby, P. R. *Angew. Chem., Int. Ed.* **1998**, *37*, 3036.

(59) Wong, W. Y.; Lu, G.-L.; Choi, K.-H.; Shi, J.-X. *Macromolecules* **2002**, *35*, 3506.

ligand-centered oxidation is not favored. In view of a more positive oxidation potential observed for a branched chloropalladium(II) complex relative to their chloroplatinum(II) analogues,⁴⁹ the involvement of a metal-centered character in the highest occupied molecular orbital (HOMO) of these d⁸ alkynyl complexes is likely. Thus, the irreversible oxidative waves of these complexes at +1.06 to +1.22 V versus SCE are likely to involve a certain degree of metal-centered character. As with the oxadiazole complexes, slightly less positive waves were observed for complexes 5–8 compared to their corresponding precursor complex 4. This observation agrees with the slight red shift observed in the lowest energy absorption bands in their respective electronic absorption spectra relative to that of their chloro precursors. Besides, reversible couples at about +0.65 V were observed for the triphenylamine-containing complexes 3 and 6. In view of the close resemblance of these couples, they are likely to be ascribed to triphenylamine-based oxidation with some mixing of metal-centered character. Similar oxidation potentials have been reported for triphenylamine-containing platinum(II) complexes.⁶⁰

Conclusion

A number of luminescent platinum(II) alkynyl complexes, $[\{RC\equiv CPt(PEt_3)_2C\equiv C\}_2\text{-oxa-2,5}]$ (where R = C₆H₄Me and (C₆H₅)₂NC₆H₄) and $[\{RC\equiv C(PEt_3)_2PtC\equiv C\}_3\text{-truxene}]$ (where R = C₆H₄Me, C₆H₄OMe, carbazole-C₆H₄, 1-methylbenzimidazole) were successfully synthesized and characterized. The electronic absorption spectra of these complexes are dominated by intraligand $[\pi\rightarrow\pi^*(C\equiv C)_2\text{-oxa-2,5}]$ or $(C\equiv C)_3\text{-truxene}]$ transitions, mixed with some $[d\pi(Pt)\rightarrow\pi^*(C\equiv C)_2\text{-oxa-2,5}]$ or $(C\equiv C)_3\text{-truxene}$ or $C\equiv CR]$ MLCT and IL $[\pi\rightarrow\pi^*(C\equiv CR)]$ character. These complexes were found to be emissive at room temperature with rich vibronic structures. Their lowest lying emissive states were assigned to be derived from ³IL states of the central oxadiazole and truxene moiety. These complexes were also found to show 2PA, and their 2PA cross-sections at excitation wavelength at 720 nm have been determined.

Experimental Section

Materials and Reagents. *trans*-Dichlorobis(triethylphosphine)-platinum(II) was obtained from Aldrich Chemical Co. 2,5-Bis-(4-ethynyl)phenyl-1,3,4-oxadiazole ((C≡C)₂-oxa-2,5),⁶¹ 10,15-dihydro-5H-diindeno[1,2-*a*;1',2'-*c*]fluorene (truxene),⁶² 9-(4-ethynylphenyl)-carbazole (carb),⁶³ (4-ethynylphenyl)diphenylamine,⁶⁴ and 2-ethynyl-1-methylbenzimidazole (bzim)⁶⁵ were synthesized according to literature procedures. Tribromohexabutyltruxene was prepared according to slight modification of a reported procedure.²²

- (60) Jones, S. C.; Coropceanu, V.; Barlow, S.; Kinnibrugh, T.; Timofeeva, T.; Brédas, J.-L.; Marder, S. R. *J. Am. Chem. Soc.* **2004**, *126*, 11782.
 (61) Dong, Y.-B.; Zhang, Q.; Wang, L.; Ma, J.-P.; Huang, R.-Q.; Shen, D.-Z.; Chen, D.-Z. *Inorg. Chem.* **2005**, *44*, 6591.
 (62) Dehmlow, E. V.; Kelle, T. *Synth. Commun.* **1997**, *27*, 2021.
 (63) Sanda, F.; Kawaguchi, T.; Masuda, T. *Macromolecules* **2003**, *36*, 2224.
 (64) Mallroy, S. P.; Cló, E.; Nikolajsen, L.; Frederiksen, P. K.; Nielsen, C. B.; Mikkelsen, K. V.; Gothelf, K. V.; Ogilby, P. R. *J. Org. Chem.* **2005**, *70*, 1134.
 (65) Satake, A.; Shoji, O.; Kobuke, Y. *J. Organomet. Chem.* **2007**, *692*, 635.

1-Indanone (Aldrich, 99+%), 1-ethynyltoluene (GFS, 98%), 1-bromobutane (Lancaster, 98+%), *n*-butyllithium (Fluka, 1.6 M solution in *n*-hexane), trimethylsilyl acetylene (GFS, 98%) and fluorescein (Acros, 99% pure, laser grade) were purchased and used as received. All solvents were purified and distilled using standard procedures before use. All other reagents were of analytical grade and were used as received.

Syntheses. Tribromohexabutyltruxene. This was synthesized according to modification of a literature procedure.²² To a solution of hexabutyltruxene (1.11 g, 1.64 mmol) in dichloromethane (15 mL) was added dropwise bromine (0.42 mL, 8.21 mmol) in dichloromethane (5 mL) over 5 min at room temperature in the dark. The mixture was then stirred for 24 h at room temperature. Excess bromine was removed by washing it with aqueous sodium thiosulfate solution. The desired product was then extracted with dichloromethane and washed successively with aqueous sodium carbonate solution and deionized water. The organic fraction was dried over anhydrous Na₂SO₄ and filtered. The crude product was obtained after solvent removal. Subsequent recrystallization of the crude product with ethanol afforded tribromohexabutyltruxene as a bright yellow solid. Yield: 1.08 g, 72%. ¹H NMR (400 MHz, CDCl₃, 298 K, relative to Me₄Si): δ 0.40–0.59 (m, 30H; ⁿBu), 0.80–0.99 (m, 12H; ⁿBu), 1.99–2.09 (m, 6H; ⁿBu), 2.81–2.91 (m, 6H; ⁿBu), 7.52 (d, 3H, *J*_{HH} = 8.5 Hz; protons at C-3, C-8, C-13), 7.57 (s, 3H; protons at C-1, C-6, C-11), 8.19 (d, 3H, *J*_{HH} = 8.5 Hz; protons at C-4, C-9, C-14). Positive-ion FAB MS: *m/z*: 917 [M + 1]⁺.

Triethynylhexabutyltruxene. This was synthesized according to a modification of a literature procedure.⁶⁶ A mixture of tribromohexabutyltruxene (1.08 g, 1.18 mmol), Pd(PPh₃)₂Cl₂ (0.12 g, 0.18 mmol), PPh₃ (0.05 g, 0.18 mmol), and CuI (0.03 g, 0.18 mmol) were suspended in diethylamine (30 mL). Trimethylsilyl acetylene (1.0 mL, 7.10 mmol) was added to the mixture, and the mixture was heated to reflux under nitrogen overnight. The solvent was then removed in vacuo. Diethyl ether was added to the organic mixture, and the diethylammonium salt was filtered off. The filtrate was evaporated under reduced pressure, and the residue was purified by column chromatography on silica gel (70–230 mesh) using hexane as the eluent to give tris(trimethylsilyl)ethynylhexabutyltruxene as a pale yellow solid after removal of the solvent. The yellow solid (0.97 g, 1 mmol) was dissolved in dichloromethane-methanol (1:1, v/v), and NaOH (1.6 g, 40 mmol) dissolved in a minimum amount of deionized water was added. The mixture was stirred under nitrogen for 2 h. The reaction was quenched by deionized water, and the organic solvent was removed under reduced pressure. It was then extracted with dichloromethane and dried over anhydrous Na₂SO₄. Subsequent recrystallization from dichloromethane-methanol afforded triethynylhexabutyltruxene as pale yellow crystalline solids. Yield: 0.72 g, 81%. ¹H NMR (400 MHz, CDCl₃, 298 K, relative to Me₄Si): δ 0.37–0.53 (m, 30H; ⁿBu), 0.77–0.98 (m, 12H; ⁿBu), 2.03–2.13 (m, 6H; ⁿBu), 2.85–2.95 (m, 6H; ⁿBu), 3.20 (s, 3H; C≡CH), 7.55 (d, 3H, *J*_{HH} = 8.2 Hz; protons at C-3, C-8, C-13), 7.59 (s, 3H; protons at C-1, C-6, C-11), 8.31 (d, 3H, *J*_{HH} = 8.2 Hz; protons at C-4, C-9, C-14). Positive-ion FAB MS: *m/z*: 751 [M]⁺.

[[CIPt(PEt₃)₂C≡C]₂-oxa-2,5] (1). This was synthesized according to a slight modification of a literature procedure with shorter reaction time.⁴⁹ *trans*-[Pt(PEt₃)₂Cl₂] (1.00 g, 1.99 mmol) and 2,5-bis-(4-ethynyl)phenyl-1,3,4-oxadiazole (0.13 g, 0.50 mmol) were dissolved in a mixture of toluene (70 mL) and piperidine (5 mL). The reaction mixture was heated to reflux for 30 min after which

- (66) Chen, Q.-Q.; Liu, F.; Ma, Z.; Peng, B.; Wei, W.; Huang, W. *Synlett* **2007**, *20*, 3145.

CuI (5 mg, 0.03 mmol) was added, and the reaction mixture was then refluxed under nitrogen for 2 days. The solvent was removed under vacuum, and the yellowish oily residue was dissolved in dichloromethane and washed successively with aqueous ammonium chloride solution and deionized water. The organic fraction was then dried over anhydrous Na_2SO_4 and filtered. The solvent was evaporated under reduced pressure. Further purification was accomplished by column chromatography on basic aluminum oxide (50–200 μm), in which the excess *trans*-[Pt(PET₃)₂Cl₂] was first eluted with dichloromethane-hexane (1:1, v/v) followed by the elution of **1** with dichloromethane. Subsequent recrystallization from dichloromethane-hexane afforded **1** as a pale yellow microcrystalline solid. Yield: 0.46 g, 77%. ¹H NMR (400 MHz, CDCl₃, 298 K, relative to Me₄Si): δ 1.17–1.27 (virtual quintet (vq), 36H, $J = 8.0$ Hz; $-\text{CH}_3$), 2.03–2.13 (m, 24H; $-\text{CH}_2\text{P}$), 7.36 (d, 4H, $J_{\text{HH}} = 8.5$ Hz; $-\text{C}_6\text{H}_4-$), 7.96 (d, 4H, $J_{\text{HH}} = 8.5$ Hz; $-\text{C}_6\text{H}_4-$). ³¹P{¹H} NMR (162 MHz, CDCl₃, 298 K, relative to 85% H₃PO₄): δ 15.10 (s, $J_{\text{Pt-P}} = 2374$ Hz). IR (KBr disk, ν/cm^{-1}): 2114 (m) $\nu(\text{C}\equiv\text{C})$. Positive-ion FAB MS: m/z : 1203 [$M + 1$]⁺. Elemental analysis calcd (%) for **1**: C 41.97, H 5.70, N 2.33; found: C 41.76, H 5.74, N 2.50.

[[MeC₆H₄C≡C Pt(PET₃)₂C≡C]₂-oxa-2,5] (**2**). This was synthesized according to a slight modification of a literature procedure.⁴⁹ Complex **1** (0.12 g, 0.10 mmol) and 1-ethynyltoluene (0.04 g, 0.30 mmol) were dissolved in a mixture of THF (20 mL) and triethylamine (10 mL). CuI (5 mg) was added to this reaction mixture as a catalyst. The yellow mixture was then stirred under nitrogen overnight at room temperature, after which the solvent was removed under reduced pressure. The yellow residue was then dissolved in dichloromethane, washed successively with brine and deionized water, and dried over anhydrous Na_2SO_4 . The solution was then filtered, and the solvent was removed under reduced pressure. The yellow residue was chromatographed on basic alumina oxide (50–200 μm) with dichloromethane as the eluent. Subsequent recrystallization of the crude product with dichloromethane-methanol afforded **2** as a yellow solid. Yield: 0.05 g, 35%. ¹H NMR (400 MHz, CDCl₃, 298 K, relative to Me₄Si): δ 1.19–1.27 (vq, 36H, $J = 8.0$ Hz; $-\text{CH}_3$), 2.15–2.22 (m, 24 H; $-\text{CH}_2\text{P}$), 2.30 (s, 6H; $-\text{C}_6\text{H}_4\text{Me}$), 7.03 (d, 4H, $J_{\text{HH}} = 8.0$ Hz; $-\text{C}_6\text{H}_4-$), 7.18 (d, 4H, $J_{\text{HH}} = 8.0$ Hz; $-\text{C}_6\text{H}_4-$), 7.38 (d, 4H, $J_{\text{HH}} = 8.4$ Hz; $-\text{C}_6\text{H}_4-$), 7.96 (d, 4H, $J_{\text{HH}} = 8.4$ Hz; $-\text{C}_6\text{H}_4-$). ³¹P{¹H} NMR (162 MHz, CDCl₃, 298 K, relative to 85% H₃PO₄): δ 11.21 (s, $J_{\text{Pt-P}} = 2363$ Hz). IR (KBr disk, ν/cm^{-1}): 2099 (m) $\nu(\text{C}\equiv\text{C})$. Positive-ion FAB MS: m/z : 1362 [$M + 1$]⁺. Elemental analysis calcd (%) for **2**: C 52.94, H 6.07, N 2.06; found: C 52.97, H 6.10, N 2.29.

[[C₆H₅]₂NC₆H₄C≡C Pt(PET₃)₂C≡C]₂-oxa-2,5] (**3**). The procedure was similar to that for **2** except that (4-ethynylphenyl)diphenylamine (0.08 g, 0.30 mmol) was used instead of 1-ethynyltoluene. Subsequent recrystallization of the crude product with dichloromethane-*n*-hexane afforded **3** as a pale yellow solid. Yield: 0.07 g, 52%. ¹H NMR (400 MHz, CDCl₃, 298 K, relative to Me₄Si): δ 1.20–1.28 (vq, 36H, $J = 8.0$ Hz; $-\text{CH}_3$), 2.15–2.23 (m, 24 H; $-\text{CH}_2\text{P}$), 6.93 (d, 4H, $J_{\text{HH}} = 8.6$ Hz; $-\text{C}_6\text{H}_4\text{NPh}_2$), 6.98 (t, 4H, $J_{\text{HH}} = 7.3$ Hz; $-\text{C}_6\text{H}_4\text{NPh}_2$), 7.07 (d, 8H, $J_{\text{HH}} = 7.6$ Hz; $-\text{C}_6\text{H}_4\text{NPh}_2$), 7.16 (d, 4H, $J_{\text{HH}} = 8.6$ Hz; $-\text{C}_6\text{H}_4\text{NPh}_2$), 7.23 (t, 8H, $J_{\text{HH}} = 7.3$ Hz; $-\text{C}_6\text{H}_4\text{NPh}_2$), 7.38 (d, 4H, $J_{\text{HH}} = 8.4$ Hz; $-\text{C}_6\text{H}_4-$), 7.96 (d, 4H, $J_{\text{HH}} = 8.4$ Hz; $-\text{C}_6\text{H}_4-$). ³¹P{¹H} NMR (162 MHz, CDCl₃, 298 K, relative to 85% H₃PO₄): δ 11.24 (s, $J_{\text{Pt-P}} = 2365$ Hz). IR (KBr disk, ν/cm^{-1}): 2099 (m) $\nu(\text{C}\equiv\text{C})$. Positive-ion FAB MS: m/z : 1668 [$M + 1$]⁺. Elemental analysis calcd (%) for **3**: C 59.14, H 5.80, N 3.36; found: C 59.20, H 5.95, N 3.35.

[[Cl(PET₃)₂PtC≡C]₃truxene] (**4**). The procedure was similar to that for **1** except that triethynylhexabutyltruxene (0.38 g, 0.50 mmol) was used instead of 2,5-bis-(4-ethynyl)phenyl-1,3,4-oxadiazole.

Subsequent recrystallization of the crude product with dichloromethane-*n*-hexane afforded **4** as a pale yellow microcrystalline solid. Yield: 0.77 g, 72%. ¹H NMR (400 MHz, CDCl₃, 298 K, relative to Me₄Si): δ 0.43–0.58 (m, 30H; ^{*n*}Bu), 0.86–0.91 (m, 12H; ^{*n*}Bu), 1.20–1.31 (vq, 54H, $J = 8.0$ Hz; $-\text{CH}_3$), 1.95–2.05 (m, 6H; ^{*n*}Bu), 2.09–2.18 (m, 36 H; $-\text{CH}_2\text{P}$), 2.82–2.92 (m, 6H; ^{*n*}Bu), 7.30 (s, 6H; protons at C-1, C-3, C-6, C-8, C-11, C-13), 8.17 (d, 3H, $J_{\text{HH}} = 8.7$ Hz; protons at C-4, C-9, C-14). ³¹P{¹H} NMR (162 MHz, CDCl₃, 298 K, relative to 85% H₃PO₄): δ 14.84 (s, $J_{\text{Pt-P}} = 2392$ Hz). IR (KBr disk, ν/cm^{-1}): 2112 (m) $\nu(\text{C}\equiv\text{C})$. Positive-ion FAB MS: m/z : 2149 [M]⁺. Elemental analysis calcd (%) for **4**: C 51.99, H 7.18; found: C 51.88, H 7.21.

[[carb-C₆H₄C≡C(PET₃)₂PtC≡C]₃truxene] (**5**). The procedure was similar to that for **2** except that complex **4** (0.22 g, 0.10 mmol) and 9-(4-ethynylphenyl)carbazole (0.11 g, 0.40 mmol) were used instead of complex **1** and 1-ethynyltoluene, respectively. Subsequent recrystallization of the crude product with dichloromethane-*n*-hexane afforded **5** as a yellowish-orange solid. Yield: 0.11 g, 40%. ¹H NMR (400 MHz, CDCl₃, 298 K, relative to Me₄Si): δ 0.43–0.61 (m, 30H; ^{*n*}Bu), 0.86–0.91 (m, 12H; ^{*n*}Bu), 1.27–1.38 (vq, 54H, $J = 8.0$ Hz; $-\text{CH}_3$), 2.00–2.09 (m, 6H; ^{*n*}Bu), 2.28–2.33 (m, 36 H; $-\text{CH}_2\text{P}$), 2.86–2.95 (m, 6H; ^{*n*}Bu), 7.28 (d, 6H, $J_{\text{HH}} = 7.7$ Hz; protons at 3,6-positions of carb), 7.30 (d, 3H, $J_{\text{HH}} = 7.7$ Hz; protons at C-3, C-8, C-13), 7.37 (s, 3H; protons at C-1, C-6, C-11), 7.40–7.42 (m, 18H; protons at 2,7-positions of carb and $-\text{C}_6\text{H}_4-$), 7.50 (d, 6H, $J_{\text{HH}} = 8.4$ Hz; protons at 1,8-positions of carb), 8.14 (d, 6H, $J_{\text{HH}} = 7.7$ Hz; protons at 4,5-positions of carb), 8.20 (d, 3H, $J_{\text{HH}} = 8.4$ Hz; protons at C-4, C-9, C-14). ³¹P{¹H} NMR (162 MHz, CDCl₃, 298 K, relative to 85% H₃PO₄): δ 11.19 (s, $J_{\text{Pt-P}} = 2371$). IR (KBr disk, ν/cm^{-1}): 2099 (m) $\nu(\text{C}\equiv\text{C})$. Positive-ion FAB MS: m/z : 2842 [$M + 1$]⁺. Elemental analysis calcd (%) for **5**: C 64.68, H 6.70, N 1.48; found: C 64.87, H 6.89, N 1.58.

[[C₆H₅]₂NC₆H₄C≡C(PET₃)₂PtC≡C]₃truxene] (**6**). The procedure was similar to that for **5** except that (4-ethynylphenyl)diphenylamine (0.11 g, 0.40 mmol) was used instead of 9-(4-ethynylphenyl)carbazole. Subsequent recrystallization of the crude product with dichloromethane-*n*-hexane afforded **6** as a yellow solid. Yield: 0.20 g, 72%. ¹H NMR (400 MHz, CDCl₃, 298 K, relative to Me₄Si): δ 0.44–0.57 (m, 30H, ^{*n*}Bu), 0.83–0.96 (m, 12H, ^{*n*}Bu), 1.24–1.31 (vq, 54H, $J = 8.0$ Hz; $-\text{CH}_3$), 1.97–2.04 (m, 6H; ^{*n*}Bu), 2.24–2.27 (m, 36H; $-\text{CH}_2\text{P}$), 2.83–2.91 (m, 6H; ^{*n*}Bu), 6.94 (d, 6H, $J_{\text{HH}} = 8.6$ Hz; $-\text{C}_6\text{H}_4-$), 6.98 (t, 6H, $J_{\text{HH}} = 7.4$ Hz; $-\text{C}_6\text{H}_4\text{NPh}_2$), 7.08 (d, 12H, $J_{\text{HH}} = 7.5$ Hz; $-\text{C}_6\text{H}_4\text{NPh}_2$), 7.17 (d, 6H, $J_{\text{HH}} = 8.6$ Hz; $-\text{C}_6\text{H}_4-$), 7.24 (t, 12H, $J_{\text{HH}} = 7.4$ Hz; $-\text{C}_6\text{H}_4\text{NPh}_2$), 7.28 (d, 3H, $J_{\text{HH}} = 8.4$ Hz; protons at C-3, C-8, C-13), 7.33 (s, 3H; protons at C-1, C-6, C-11), 8.16 (d, 3H, $J_{\text{HH}} = 8.4$ Hz; protons at C-4, C-9, C-14). ³¹P{¹H} NMR (162 MHz, CDCl₃, 298 K, relative to 85% H₃PO₄): δ 11.06 (s, $J_{\text{Pt-P}} = 2375$ Hz). IR (KBr disk, ν/cm^{-1}): 2097 (m) $\nu(\text{C}\equiv\text{C})$. Positive-ion FAB MS: m/z : 2848 [$M + 1$]⁺. Elemental analysis calcd (%) for **6**: C 64.54, H 6.90, N 1.48; found: C 64.25, H 6.96, N 1.53.

[[CH₃C₆H₄C≡C(PET₃)₂PtC≡C]₃truxene] (**7**). The procedure was similar to that for **5** except that 1-ethynyltoluene (0.05 g, 0.40 mmol) was used instead of 9-(4-ethynylphenyl)carbazole. Subsequent recrystallization of the crude product with dichloromethane-methanol afforded **7** as a yellow solid. Yield: 0.18 g, 73%. ¹H NMR (400 MHz, CDCl₃, 298 K, relative to Me₄Si): δ 0.44–0.56 (m, 30H; ^{*n*}Bu), 0.87–0.94 (m, 12H; ^{*n*}Bu), 1.25–1.31 (vq, 54H, $J = 8.0$ Hz; $-\text{CH}_3$), 1.98–2.04 (m, 6H; ^{*n*}Bu), 2.24–2.26 (m, 36H; $-\text{CH}_2\text{P}$), 2.27 (s, 9H; $-\text{C}_6\text{H}_4\text{Me}$), 2.83–2.93 (m, 6H; ^{*n*}Bu), 7.03 (d, 6H, $J_{\text{HH}} = 8.0$ Hz; $-\text{C}_6\text{H}_4-$), 7.20 (d, 6H, $J_{\text{HH}} = 8.0$ Hz; $-\text{C}_6\text{H}_4-$), 7.28 (d, 6H, $J_{\text{HH}} = 8.4$ Hz; protons at C-1, C-3, C-6, C-8, C-11, C-13), 8.16 (d, 3H, $J_{\text{HH}} = 8.4$ Hz; protons at C-4,

C-9, C-14). $^{31}\text{P}\{^1\text{H}\}$ NMR (162 MHz, CDCl_3 , 298 K, relative to 85% H_3PO_4): δ 11.03 (s, $J_{\text{Pt-P}} = 2362$ Hz). IR (KBr disk, ν/cm^{-1}): 2100 (m) $\nu(\text{C}\equiv\text{C})$. Positive-ion FAB MS: m/z : 2389 $[M + 1]^+$. Elemental analysis calcd (%) for **7**: C 60.36, H 7.35; found: C 60.60, H 7.33.

[[bzimC≡C(PEt₃)₂PtC≡C]₃truxene] (8). The procedure was similar to that for **2** except that 2-ethynyl-1-methylbenzimidazole (0.06 g, 0.40 mmol) was used instead of 9-(4-ethynylphenyl)carbazole. Subsequent recrystallization of the crude product with dichloromethane-methanol afforded **8** as a pale orange solid. Yield: 0.13 g, 53%. ^1H NMR (400 MHz, CDCl_3 , 298 K, relative to Me_4Si): δ 0.45–0.60 (m, 30H; ^nBu), 0.83–0.95 (m, 12H; ^nBu), 1.24–1.32 (vq, 54H, $J = 8.0$ Hz; $-\text{CH}_3$), 1.99–2.06 (m, 6H; ^nBu), 2.24–2.28 (m, 36H; $-\text{CH}_2\text{P}$), 2.85–2.92 (m, 6H; ^nBu), 3.83 (s, 9H; $-\text{CH}_3$ at bzim), 7.23 (s, 9H; protons at 4, 5 and 6-positions at bzim), 7.30 (d, 3H, $J_{\text{HH}} = 8.1$ Hz; protons at C-3, C-8, C-13), 7.35 (s, 3H; protons at C-1, C-6, C-11), 7.70 (d, 3H, $J_{\text{HH}} = 8.3$ Hz; protons at 7-position of bzim), 8.19 (d, 3H, $J_{\text{HH}} = 8.1$ Hz; protons at C-4, C-9, C-13). $^{31}\text{P}\{^1\text{H}\}$ NMR (162 MHz, CDCl_3 , 298 K, relative to 85% H_3PO_4): δ 11.71 (s, $J_{\text{Pt-P}} = 2353$ Hz). IR (KBr disk, ν/cm^{-1}): 2101 (m) $\nu(\text{C}\equiv\text{C})$. Positive-ion FAB MS: m/z : 2510 $[M]^+$. Elemental analysis calcd (%) for **8**: C 59.03, H 7.07, N 3.33; found: C 59.34, H 7.34, N 3.08.

Physical Measurements and Instrumentation. ^1H NMR spectra were recorded on Bruker DPX 300 (300 MHz) or Bruker DPX 400 (400 MHz) Fourier-transform NMR spectrometers with chemical shifts reported relative to tetramethylsilane, Me_4Si , while $^{31}\text{P}\{^1\text{H}\}$ spectra were recorded either on a Bruker DPX 400 or a Bruker DPX 500 Fourier-transform NMR spectrometer with chemical shifts reported relative to 85% H_3PO_4 . Positive-ion FAB mass spectra were recorded on Finnigan MAT95 mass spectrometer. IR spectra were obtained using KBr disks on a Bio-Rad FTS-7 Fourier-Transform infrared spectrophotometer (4000–400 cm^{-1}). Elemental analyses were performed on a Flash EA 1112 elemental analyzer at the Institute of Chemistry, Chinese Academy of Sciences. The electronic absorption spectra were obtained by using a Hewlett-Packard 8452 A diode array spectrophotometer. Steady-state excitation and emission spectra at room temperature and at 77 K were recorded on a Spex Fluorolog-2 Model F111 fluorescence spectrofluorometer. Solid-state photophysical studies were carried out with solid samples contained in a quartz tube inside a quartz-walled Dewar flask. Measurements of the ethanol-methanol (4:1, v/v) glass or solid-samples at 77 K were conducted by using liquid nitrogen filled in the optical Dewar flask. All solutions for photophysical studies were degassed with a high-vacuum line on a two-compartment cell consisting of a 10 mL Pyrex bulb and a quartz cuvette (1 cm path length) and sealed from the atmosphere by a Bibby Rotaflo HP6 Teflon stopper. The solutions were rigorously degassed with at least four successive freeze–pump–thaw cycles. Emission lifetime measurements were performed by using a conventional laser system. The excitation source was with a 355 nm output (third harmonic) from a Spectra-Physics Quanta-Ray Q-switch GCR-150-10 pulsed Nd:YAG laser. Luminescence decay signals were detected by a Hamamatsu R928 photomultiplier tube, recorded on a Tektronix Model TDS-620 A (500 MHz, 2 GS s^{-1}) digital oscilloscope, and analyzed by using a program for exponential fits.

The 2PA cross-section (σ_2) can be determined by two main methods.^{67,68} Two-photon induced luminescence (TPIL) is one of the methods to determine σ_2 in which the luminescence intensity generated by 2PA was measured and used to estimate the σ_2 values

according to eq 1. An unknown sample is compared to a reference with known σ_2 values. Fluorescein (1×10^{-4} M in 0.1 M NaOH aqueous solution) was used as the reference in the present study.⁶⁹

$$\sigma_{2(s)} = \frac{C_r n_r \Phi_r S_s}{C_s n_s \Phi_s S_r} \sigma_{2(r)} \quad (1)$$

where σ_2 is the 2PA cross-section, C is the concentration, n is refractive index, Φ is the luminescence quantum yield, and S is the integrated luminescence signal. The subscripts r and s represent the reference and the sample material, respectively. The σ_2 and luminescence quantum yield of fluorescein in 0.1 M NaOH solution (pH \sim 11) at 720 nm were assumed to be 19 GM (Göppert-Mayer, 1 GM = 1×10^{-50} $\text{cm}^4 \text{ sec photon}^{-1} \text{ molecule}^{-1}$) and 0.90,⁶⁹ respectively. The time-averaged laser power at 720 nm was kept constant for the sample and the reference. The laser pulses were generated by a mode-locked Ti:Sapphire laser (Spectra-Physics, Tsunami) operating at a repetition rate of 85 MHz. The pulses were amplified up to 1 mJ per pulse by the Ti:Sapphire regenerative amplifier (Spectra-Physics, Spitfire) with pulse duration of \sim 120 fs and repetition rate of 1 kHz. The 720 nm laser output from the OPA (Coherent, TOPAS-C light conversion) was used as the excitation source. The laser output was passed through the sample cell, and the luminescence intensity was monitored by the spectrometer system with monochromator (ACTON Research Corporation, SpectraPro 2300i) and photomultiplier tube (Hamamatsu, R636-10). For the power dependence measurements, the laser beam power was altered by using two polarizers, which was partially reflected to a photodiode for the monitoring of the excitation power. The experimental setup for the two-photon induced luminescence studies is shown in Figure 6.

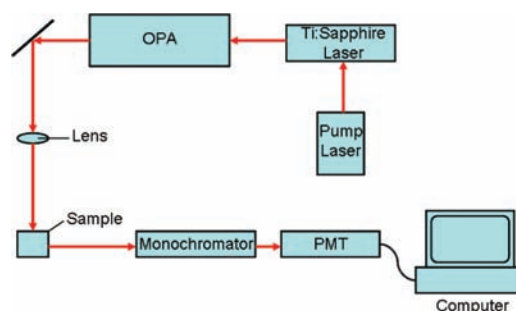


Figure 6. Schematic experimental setup for two-photon induced luminescence (TPIL) measurement.

Cyclic voltammetric measurements were performed using a CH Instruments, Inc., model CHI 750 A electrochemical analyzer. Electrochemical measurements were performed in dichloromethane solutions with 0.1 M $^n\text{Bu}_4\text{NPF}_6$ (TBAH) as the supporting electrolyte at room temperature. The reference electrode was an Ag/AgNO₃ (0.1 M in acetonitrile) electrode, and the working electrode was a glassy carbon electrode (CH Instruments, Inc.) with a platinum wire as the counter electrode. The working electrode surface was first polished with 1 μm alumina slurry (CH Instruments, Inc.) and then with 0.3 μm alumina slurry (CH Instruments, Inc.) on a microcloth (Buehler Co.). It was rinsed with ultrapure deionized water and sonicated in a beaker containing ultrapure

(67) Xu, C.; Webb, W. W. Multiphoton Excitation of Molecular Fluorophores and Nonlinear Laser Microscopy. In *Topics in Fluorescence Spectroscopy*; Lakowicz, J. R., Ed.; Plenum Press: New York, 1997; Vol. 5, Chapter 11, pp 471–537.

(68) Xu, C.; Webb, W. W. *J. Opt. Soc. Am. B* **1996**, *13*, 481.

(69) Albota, M. A.; Xu, C.; Webb, W. W. *Appl. Opt.* **1998**, *37*, 7352.

deionized water for 5 min. The polishing and sonicating steps were repeated twice and then the working electrode was rinsed under a stream of ultrapure deionized water. The ferrocenium/ferrocene couple ($\text{FeCp}_2^{+/0}$) was used as the internal reference. All solutions for electrochemical studies were deaerated with prepurified argon gas prior to measurements.

X-ray Crystal Structure Determination. Crystals of triethynylhexabutyltruxene were obtained by recrystallization from dichloromethane-methanol. Crystal data: $[\text{C}_{57}\text{H}_{66}]$, $M = 751.10$, orthorhombic, space group $Pna2_1$, $a = 16.570(3) \text{ \AA}$, $b = 18.708(4) \text{ \AA}$, $c = 15.787(3) \text{ \AA}$, $V = 4893.8(17) \text{ \AA}^3$, $Z = 4$, $D_c = 1.019 \text{ g cm}^{-3}$, $\mu(\text{Mo K}\alpha) = 0.057 \text{ mm}^{-1}$, $F(000) = 1632$, $T = 301 \text{ K}$. A pale yellow crystal of dimensions $0.6 \text{ mm} \times 0.4 \text{ mm} \times 0.25 \text{ mm}$ in a glass capillary was used for data collection at $28 \text{ }^\circ\text{C}$ on a MAR diffractometer with a 300 mm image plate detector using graphite monochromatized Mo $\text{K}\alpha$ radiation ($\lambda = 0.71073 \text{ \AA}$). Data collection was made with 1.5° oscillation step of φ (120 images) at 120 mm distance and 5 min exposure. The images were interpreted and intensities integrated using program DENZO.⁷⁰ The structure was solved by direct methods by employing the SHELXS-97 program⁷¹ on a PC. Most C atoms were located according to the direct methods. The positions of the other non-hydrogen atoms were found after successful refinement by full-matrix least-squares using program SHELXL-97⁷² on a PC. There was one formula unit in the asymmetric unit. Two *n*-butyl groups were disordered into two sets of positions. Restraints were applied to the disordered C atoms, assuming similar C–C and 1,3-C•••C bond lengths or distances, respectively. According to the SHELXL-97 program,⁷² all 8174 independent reflections (R_{int}^{73} equal to 0.0645, 3199 reflections larger than $4\sigma(F_o)$) from a total of 32031 reflections participated in the full-matrix least-squares refinement against F^2 . These reflections were in the range $-17 \leq h \leq 18$, $-22 \leq k \leq 22$, $-19 \leq l \leq 18$ with $2\theta_{\text{max}}$ equal to 51.30° . In the final stage of least-squares refinement, disordered C atoms were refined isotropically; other non-H atoms were refined anisotropically. H atoms

were generated by program SHELXL-97 program⁷² and were calculated based on the riding mode with thermal parameters equal to 1.2 times that of the associated C atoms and participated in the calculation of final R -indices. Since the structure refinements are against F^2 , R -indices based on F^2 are larger than (more than double) those based on F . For comparison with older refinements based on F and an OMIT threshold, a conventional index R_1 based on observed F values larger than $4\sigma(F_o)$ is also given (corresponding to Intensity $\geq 2\sigma(I)$). $wR_2 = \{\sum[w(F_o^2 - F_c^2)^2]/\sum w(F_o^2)^2\}^{1/2}$, $R_1 = \sum||F_o| - |F_c||/\sum|F_o|$. The goodness of fit (GoF) is always based on F^2 : $\text{GoF} = S = \{\sum[w(F_o^2 - F_c^2)^2]/(n - p)\}^{1/2}$, where n is the number of reflections and p is the total number of parameters refined. The weighting scheme is $w = 1/[\sigma^2(F_o^2) + (aP)^2 + bP]$, where P is $[2F_c^2 + \max(F_o^2, 0)]/3$. Convergence $((\Delta/\sigma)_{\text{max}} = 0.001$, av. 0.001) for 465 variable parameters by full-matrix least-squares refinement on F^2 reaches to $R_1 = 0.0597$ and $wR_2 = 0.1396$ with a goodness-of-fit of 0.81; the parameters a and b for weighting scheme are 0.0307 and 0.0. The final difference Fourier map shows maximum rest peaks and holes of 0.165 and $-0.145 \text{ e } \text{\AA}^{-3}$, respectively. Selected bond lengths and angles are summarized in Table 1.

Acknowledgment. V.W.-W.Y. acknowledges support from The University of Hong Kong under the Distinguished Research Achievement Award Scheme. We also acknowledge support from the University Development Fund and the Faculty Development Fund of The University of Hong Kong, and the URC Strategic Research Theme on Molecular Materials. The work described in this paper has been supported by a RGC Central Allocation Vote (CAV) Grant (HKU 2/05C). C.K.M.C. acknowledges support from The University of Hong Kong and the receipt of a University Postgraduate Studentship. C.-H.T. acknowledges support from The University of Hong Kong and the receipt of a University Postdoctoral Fellowship.

Supporting Information Available: Tables of crystal data, atomic coordinates, thermal parameters, and a full list of bond distances and angles for triethynylhexabutyltruxene. This material is available free of charge via the Internet at <http://pubs.acs.org>.

IC8017979

- (70) Otwinowski, Z.; Minor, W. Processing of X-ray Diffraction Data Collected in Oscillation Mode. In *Methods in Enzymology*, Vol. 276: *Macromolecular Crystallography Part A*; Carter, C. W., Jr.; Sweet, R. M., Eds.; Academic Press: San Diego, 1997; pp 307–326.
- (71) Sheldrick, G. M. *SHELXS97, Programs for Crystal Structure Analysis*, Release 97-2; University of Göttingen: Göttingen, Germany.
- (72) Sheldrick, G. M. *SHELXL97 Programs for Crystal Structure Analysis*, Release 97-2; University of Göttingen: Göttingen, Germany.
- (73) $R_{\text{int}} = \sum|F_o^2 - F_o^2(\text{mean})|/\sum|F_o^2|$.